Experimental Section

Infrared spectra were recorded on a Perkin-Elmer 137B and/or a Beckman Acculab-6 spectrometer. The solvent was carbon tetrachloride in all cases. NMR spectra were recorded on a Varian T60-1A spectrometer with CCl_4 as solvent and tetramethylsilane as reference. The mass spectra were recorded on a Du Pont 21-490B mass spectrometer. High-resolution NMR spectra were obtained on a Varian HR-220 spectrometer operated by the Consortium at The Rockefeller University in New York.

Materials. 1,4-cyclohexadiene from Chemical Samples Co. (Columbia, OH) was carefully fractionated before use. It had ∼1% of benzene as the only impurity. 1,4-cyclohexadiene-*3,3,6,6*-d_4 was obtained from Merck and Co., Inc. It was made from the oxidation of the Diels–Alder adduct of 1,3-butadiene-*1,1,4,4*-d_4 to maleic anhydride. Its isotopic purity as determined by its NMR spectrum was >98%. It was used as obtained. Pentane (Baker-Photrex grade) was uniformly used as the solvent for photolysis.

Apparatus. Preparative photolysis at 185 nm was carried out in an annular quartz (Suprasil) reactor (Srinivasan type K) fitted with a 35-W hot cathode mercury resonance lamp.[25] In quantitative studies, the source of light was a Hanovia Ottawa-style cold cathode resonance lamp which was filtered by an Acton 185 band-pass filter to remove the radiation at 254 nm. For irradiation with 214-nm radiation, a Phillips Zn resonance lamp was used.

Procedure. Preparative Photolysis. 1,4-cyclohexadiene (0.5 g) was dissolved in 160 mL of pentane and the solution degassed with nitrogen. Irradiation in the apparatus described above was carried out at ∼20 °C for 90 min. The solution was analyzed by GLC on a Perkin-Elmer 3920 B gas chromatograph fitted with a oxydiisopropionitrile column (12 ft × $^{1}/_{4}$ in.). At the end of this period, irradiation was stopped although the conversion was only ∼50% in order to avoid secondary photolysis of the products. The solvent was removed by distillation on a 12-in. spinning-band column. The residue was separated by gas chromatography into its component products and unreacted 1,4-cyclohexadiene. For yields, see Table I. Products were identified by comparison of their IR and NMR spectra to those of authentic materials.

The workup was identical during photolysis with 214-nm radiation.

Quantitative Studies. A solution of freshly distilled 1,4-cyclohexadiene (5×10^{-2} M) in pentane was placed in a cylindrical (2.5 cm diameter × 2 cm long) quartz cell with a Suprasil window and degassed with nitrogen. The lamp was operated through a constant voltage power supply and allowed to warm up in a slow stream of nitrogen in order to stabilize its light output. The Acton filter was placed in the optical path just at the commencement of the photolysis in order to minimize its destruction. During photolysis, samples were removed at 20-min intervals and analyzed by GLC using a flame-ionization detector. The photolysis was continued until sufficient data were accumulated to provide a satisfactory linear product formation curve vs. time for each of the products. The net conversion of the starting material was ∼3%.

The light source was calibrated by the photolysis of *cis*-cyclooctene in the same apparatus.[6]

Sensitized Photolysis. The experiment with Hg atoms as sensitizer was carried out in a 5-L bulb with a central well in which a single 8-W mercury resonance lamp was placed. The bulb was evacuated and filled with 6 torr of 1,4-cyclohexadiene vapor and a drop of mercury. Photolysis was >60% complete in 60 min. Products and unreacted starting material were isolated by GLC and identified as before.

Pyrolysis of 1,4-Cyclohexadiene-*3,3,6,6*-d_4 (4). A sample of **4** (250 μL liquid) was placed in an evacuated 100 mL Pyrex bulb and pyrolyzed at 330 °C for 80 min. GC analysis showed that the material was 70% converted, and the major product (>90%) was benzene. It was separated and its mass spectrum was used as a reference for benzene-*1,4*-d_2.

Acknowledgment. This work was supported in part by Grant No. CHE-8015355 from the National Science Foundation.

---

(25) Srinivasan, R.; White, L. S. *J. Am. Chem. Soc.* **1979**, *101*, 6389.

A Kinetic Scheme for Intramolecular Excimer Formation in Bis(α-naphthylmethyl) Ether, Involving Different Starting Conformations[†]

R. Todesco, J. Gelan, H. Martens, J. Put,* and F. C. De Schryver*

Contribution from the University Centre of Limburg, Universitaire Campus, B-3610 Diepenbeek, Belgium, and the Department of Chemistry, Catholic University of Leuven, Celestijnenlaan 200F, B-3030 Heverlee, Belgium. *Received February 17, 1981. Revised Manuscript Received April 28, 1981*

Abstract: Fluorescence measurements under nonstationary conditions suggest that the intramolecular excimer formation in bis(α-naphthylmethyl) ether does not follow a simple kinetic scheme. Two excimers can be formed, an endo and an exo one, which have the same spectral distribution. In these excimers, the two naphthyl rings are parallel but most probably displaced with respect to each other. Besides fluorescence and radiationless deactivation, the excimers undergo reaction to an endo and an exo cyclomer, respectively. In isooctane, acetonitrile, and MTHF, the decay of the monomer fluorescence can be analyzed as a sum of two exponentials and the decay in the excimer region as a difference of two exponentials. However, the decay parameters of the excimer do not match those of the monomer fluorescence, indicating that back-reaction from the excimer to the monomer is slow in the whole temperature region measured. Preparative experiments yield evidence that the two components in the monomer region are most probably related to two sets of conformations, leading to exo and endo excimers, respectively, with different rates. A kinetic scheme involving these conformational aspects is proposed.

Intramolecular excimer formation in bichromophoric systems requires conformational changes in the linking chain, to allow the chromophores to approach each other. Until recently, the dependence of intramolecular complex formation on the conformation of bichromophoric molecules prior to excitation was not taken into consideration and a scheme analogous to that of the intermolecular process, as first proposed by Förster, was used.[1-10] An effect of ground-state conformations on intramolecular exciplex formation was described recently in α-phenyl-ω-dimethyl-

---

[†] Dedicated to George S. Hammond on the occasion of his 60th birthday.

* Address correspondence as follows: J.P., University Centre of Limburg; F.C.D.S., Catholic University of Leuven.

(1) B. Stevens and M. J. Ban, *Trans. Faraday Soc.*, **60**, 1515 (1964).

(2) F. Hirayama, *J. Chem. Phys.*, **42**, 3163 (1965).

(3) H. Braun and Th. Förster, *Z. Phys. Chem.* (*Wiesbaden*), **78**, 40 (1971).

(4) E. A. Chandross and C. J. Dempster, *J. Am. Chem. Soc.*, **92**, 3587 (1970).

(5) W. Klöppfer in "*Organic Molecular* Photophysics I", J. B. Birks, Ed., Wiley, New York, 1973.

(6) G. E. Johnson, *J. Chem. Phys.*, **61**, 3002 (1974).

(7) M. H. Hin and W. R. Ware, *J. Am. Chem. Soc.*, **98**, 4722 (1976).

0002-7863/81/1503-7304$01.25/0 © 1981 American Chemical Society

Table I. Photophysical Constants of II at Room Temperature

solvent	ϕ_{FMod}	τ_{Mod}, ns	$10^6 k_{\mathrm{FM}}$, s^{-1}	$10^7 k_{\mathrm{FM}}{}^0$, s^{-1}	$10^7 k_{\mathrm{IM}}{}^0$, s^{-1}	$10^7 A_{\mathrm{IM}}$, s^{-1}	E_{IM}, kJ mol^{-1}
isooctane	0.080	38.8	2.3	0.12	0.14	4.0	1.50
MTHF	0.075	28.0	2.6	0.14	0.09	8.4	2.35
CH_3CN	0.080	33.8	2.4	0.13	*a*	5.3	1.40

[a] Could not be obtained as no measurements are possible in CH_3CN at sufficiently low temperatures.

amino)alkanes[11] and β-naphthylalkylamines.[12] The effect showed up on analysis of the fuorescence decay by single photon counting. A slow decaying component was present in the monomer region, whose lifetime was longer than that of the exciplex. To explain this, a kinetic scheme was proposed, involving two sets of conformations, differing by the orientation of the amino group with respect to the chain. In this way, a set of conformations, favorable for intramolecular complex formation, is separated from a set of unfavorable conformations by an appreciable energy barrier. Deviations from the classical scheme of excimer formation were also observed by Zachariasse[13] and Halpern.[14] Morawetz[15] and co-workers used intramolecular excimer formation to study conformational transitions. In this study, they measured the fluorescence under stationary conditions of a series of dinaphthyl compounds, including bis(α-naphthylmethyl) ether.

They used a kinetic scheme involving different conformations of the linking chain, but they did not take into account the orientation of the naphthyl rings. They introduced a factor, α, the fraction of the monomer in a conformation from which a single hindered rotation can lead to excimer formation. For the bichromophoric ether, they derived an activation energy for excimer formation from the stationary results, equal to 17.5 kJ mol^{-1} in heptane as well as in ethanol. In this paper, the results are presented of a study under stationary and nonstationary conditions of bis(α-naphthylmethyl) ether, in a temperature range from −70 to +10 °C, in order to see whether the nonstationary results would confirm the interpretation of the stationary results. As a model compound, the monofunctional (α-naphthylmethyl) ethyl ether was used and it was assumed that, apart from the rate constant for excimer formation, the rate constants for the locally excited state of the bifunctional compound would equal those of the model compound.

Results and Discussion

Absorption Spectra. The UV absorption spectra of bis(α-naphthylmethyl) ether (I) and the model compound (α-naphthylmethyl) ethyl ether (II) show the same course in all three solvents studied: isooctane, 2-methyltetrahydrofurane, and acetonitrile. In Figure 1 the absorption spectra of I and II in isooctane are compared. The maxima are independent of the solvent. A close analysis of the spectra revealed that in I, the $^1L_a \leftarrow {}^1A$ band is very slightly shifted (1.5 nm) to bathochromic wavelengths. Also the molar extinction coefficiënt of I is not exactly doubled with respect to II. There is a slight hypochromism between 250 and 280 nm, and a slight hyperchromism between 285 and 305 nm, but at longer wavelengths the spectra coincide. The absorption spectra of I and II were recorded at various temperatures in all three solvents (−40 to +90 °C). No splitting of bands or shift occurred: the only effect is an increase in vibronic structure at lower temperature. On the bais of these absorption spectra one can conclude that no strong interaction between the naphthalene chromophores in the ground state exists in either solvent used.

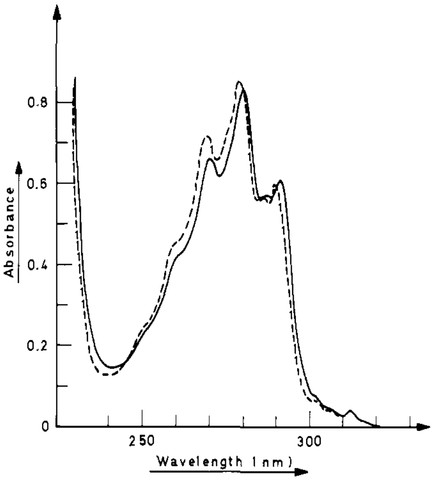

Figure 1. UV absorption spectra of bis(α-naphthylmethyl) ether (—) and (α-naphthylmethyl) ethyl ether (---) in isooctane.

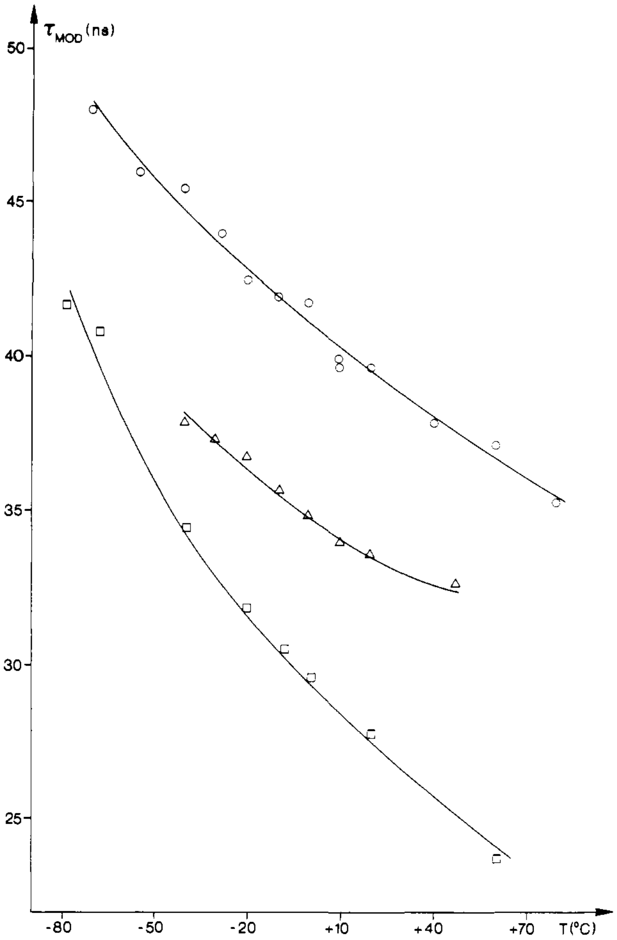

Figure 2. Fluorescence lifetimes of II vs. temperature: ○, isooctane; □, MTHF; △, CH_3CN.

---

(8) F. C. De Schrijver, N. Boens, and J. Put, *Adv. Photochem.*, **10**, 359 (1977).

(9) K. A. Zacchariasse and A. Weller, *Chem. Phys. Lett.*, **52**, 375 (1978).

(10) J. Huybrechts, M. Van der Auweraer, J. C. Dederen, N. Boens, and F. C. De Schrijver, Proceedings of the 8th IUPAC Symposium on Photochemistry, Leuven, 1978, p 188.

(11) (a) M. Van der Auweraer, A. Gilbert, and F. C. De Schryver, *Nouv. J. Chim.*, **4**, 153 (1980). (b) *J. Am. Chem. Soc.*, **100**, 1172 (1980).

(12) F. Meeus, M. Van der Auweraer, and F. C. De Schryver, *Chem. Phys. Lett.*, **74**, 218 (1980).

(13) K. Zachariasse, personal communications.

(14) A. M. Halpern, M. W. Legenza, and B. R. Ramachandran, *J. Am. Chem. Soc.*, **101**, 5736 (1979).

(15) M. Goldenberg, J. Emert, and H. Morawetz, *J. Am. Chem. Soc.*, **100**, 7171 (1978).

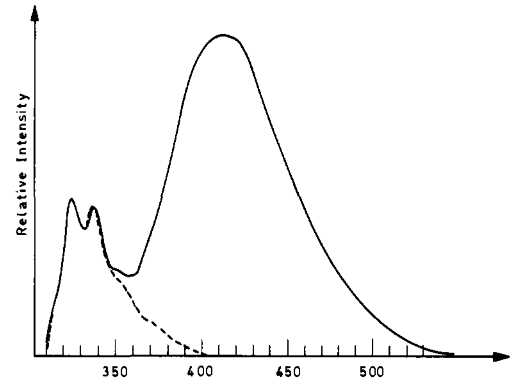

Figure 3. Fluorescence spectra of I (—) and II (---) in isooctane.

Scheme I

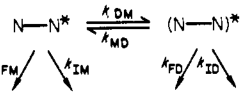

Fluorescence of the Model Compound. The fluorescence spectrum of II is typical of a locally excited α-substituted naphthalene with maxima at 321 and 336 nm[15] in all three solvents. The quantum yield of fluorescence, ϕ_{FMod}, varies with the solvent (see Table I) and the temperature. The fluorescence decay was measured by using the SPC technique and was found to be monoexponential in all solvents at all temperatures. The lifetimes, obtained by analysis of the decays, are presented in Figure 2. From these lifetimes, the fluorescence rate constants, k_{FM}, were calculated and a value of $k_{FM}{}^0$ was obtained, taking into account the refractive index.[16,17] The rate constant for nonradiative decay, k_{IM}, was found to be the sum of a temperature-independent component, $k_{IM}{}^0$, and a temperature-dependent component $k_{IM}{}'$.[18] The values of the various photophysical constants of II at room temperature in the three solvents are summarized in Table I.

Fluorescence of II under Stationary Conditions. As described earlier[15,19] the fluorescence spectrum of I shows emission from locally excited naphthalene and a broad structureless emission attributed to an excimer (Figure 3). The structure and maximum of the excimer emission can be determined from difference spectra between II and I, after normalization at the O–O transition. The position of the maximum is at 412 nm and is solvent independent and slightly temperature dependent. In isooctane the maximum of the excimer emission varies from 417 nm at -50 °C to 408 nm at +85 °C. Figure 4 shows a plot of the logarithm of the ratio of the quantum yields ϕ_{FD}/ϕ_{FM} in excimer and monomer regions, vs. $1/T$. These Stevens–Ban plots can have a "low-temperature region" where the ratio ϕ_{FD}/ϕ_{FM} increases with increasing temperature, a "high-temperature region" where the ration decreases with temperature, and a maximum at intermediate temperatures.

If Scheme I were valid in this intramolecular case, the curves in Figure 4 would be described by eq 1.[16] The tangent at the curve at low temperatures is then given by eq 2. Usually E_D is

$$\frac{\phi_{FD}}{\phi_{FM}} = \frac{k_{FD}k_{DM}}{k_{FM}(k_{MD} + k_D)} \qquad k_D = k_{FD} + k_{ID} \tag{1}$$

$$\frac{d \ln (\phi_{FD}/\phi_{FM})}{d(1/T)} = -\frac{E_{DM} - E_D}{R} \tag{2}$$

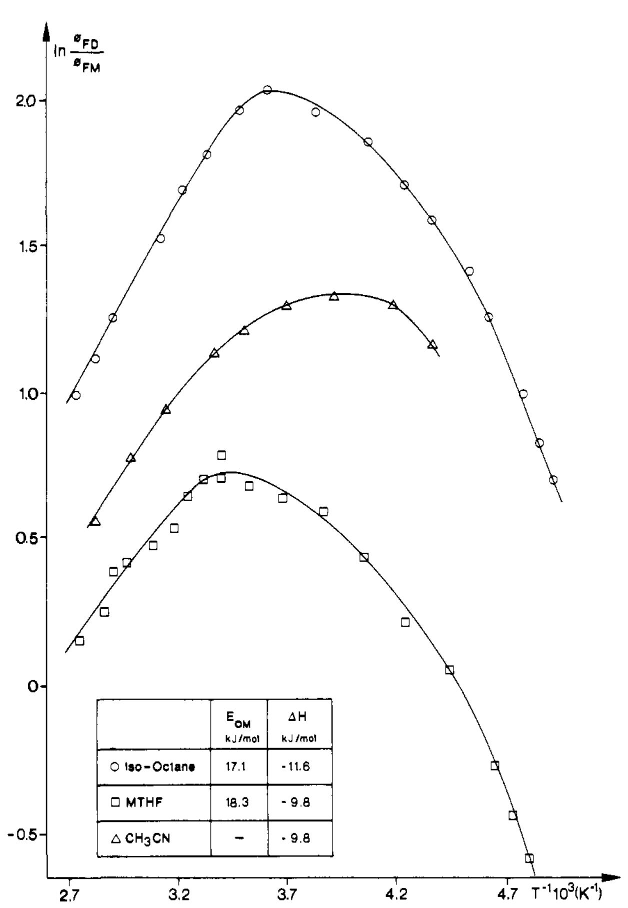

	E_{DM} kJ/mol	ΔH kJ/mol
○ Iso-Octane	17.1	-11.6
□ MTHF	18.3	- 9.8
△ CH_3CN	–	- 9.8

Figure 4. Plot of the logarithm of the ratio of fluorescence quantum yields in excimer and monomer region vs. $1/T$: ○, isooctane; □, MTHF; △, CH_3CN.

assumed to be much smaller than E_{DM}, so the slope yields the activation energy for excimer formation, E_{DM}. The tangent at the curve in the high-temperature region yields the enthalpy of excimer formation (eq 3), if it can be assumed that $k_{MD} \gg k_D$

$$\frac{d \ln (\phi_{FD}/\phi_{FM})}{d(1/T)} = -\Delta H/R \tag{3}$$

and thus that the temperature dependence of k_D is not important. Values of E_{DM} and ΔH obtained in this way from the stationary results are shown in Figure 4.

Fluorescence of I under Nonstationary Conditions. If Scheme I is valid, the time evolution of the emission from the locally excited state, $I_M(t)$, and from the excimer, $I_D(t)$, can be described by eq 4–7.[16] At intermediate temperatures, the emission in the monomer region should decay biexponentially, λ_1 and λ_2 being the two decay parameters in the monomer region and A reflecting their respective contributions. The excimer emission is in this case described as a difference of two exponentials, with the same decay parameters.

$$I_M(t) = k_{FM}\frac{\lambda_2 - X}{\lambda_2 - \lambda_1}[\exp(-\lambda_1 t) + A \exp(-\lambda_2 t)] \tag{4}$$

$$I_D(t) = \frac{k_{FD}k_{DM}}{\lambda_2 - \lambda_1}[\exp(-\lambda_1 t) - \exp(-\lambda_2 t)] \tag{5}$$

$$A = \frac{X - \lambda_1}{\lambda_2 - X} \tag{6}$$

$$X = \frac{1}{\tau_{F_{Mod}}} + k_{DM} \tag{7}$$

$$\lambda_{1,2} = \tfrac{1}{2}[(X + Y) \mp \sqrt{(Y - X)^2 + 4k_{DM}k_{MD}}]$$

To check this scheme, the time evolution of the emission in the monomer region ($\lambda_{anal} = 325$ nm) and in the excimer region (λ_{anal}

---

(16) J. B. Birks in "Photophysics of Aromatic Molecules", Wiley, Lodon, 1970, p 312.

(17) B. L. Johnson and J. Smith in "Light Scattering from Polymer Solutions", M. B. Huglin, Ed., Academic Press, London, 1972, Chapter 2, p 27.

(18) P. F. Jones and A. R. Colloway, *J. Chem. Phys.*, special issue, 110 (1969).

(19) R. S. Davidson and T. D. Whelan, *J. Chem. Soc., Chem. Commun.*, 361 (1977).

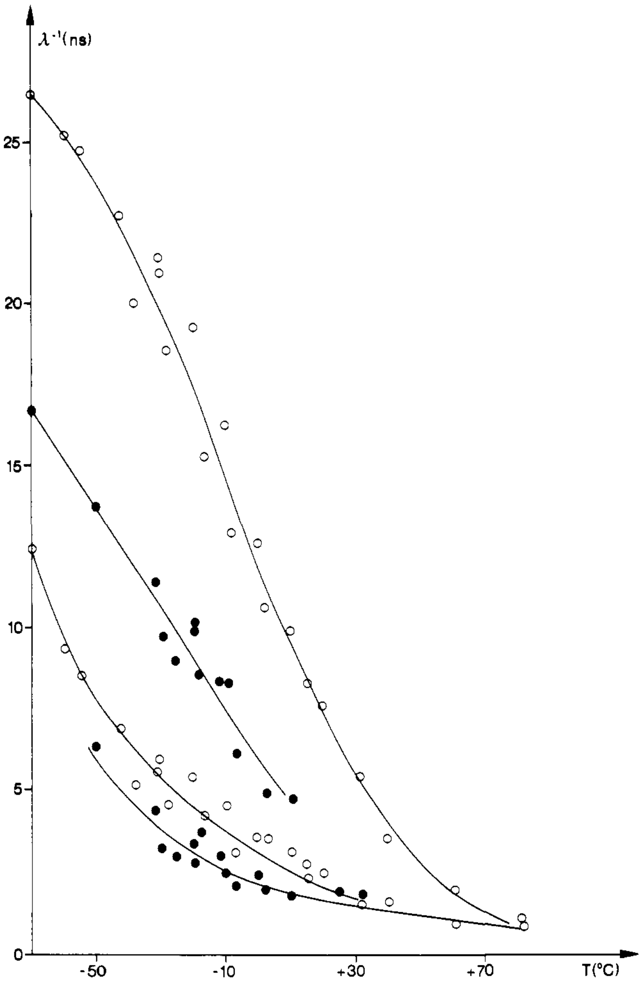

Figure 5. Fluorescence lifetimes of I in isooctane: ●, monomer region; ○, excimer region.

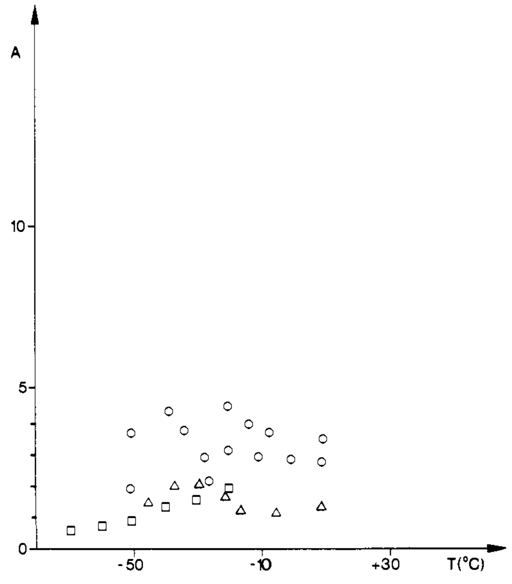

Figure 6. Contribution of the two components in the monomer region. *A* is the ratio of the preexponential term of the short living component to that of the long living component: ○, isooctane; □, MTHF; △, CH_3CN.

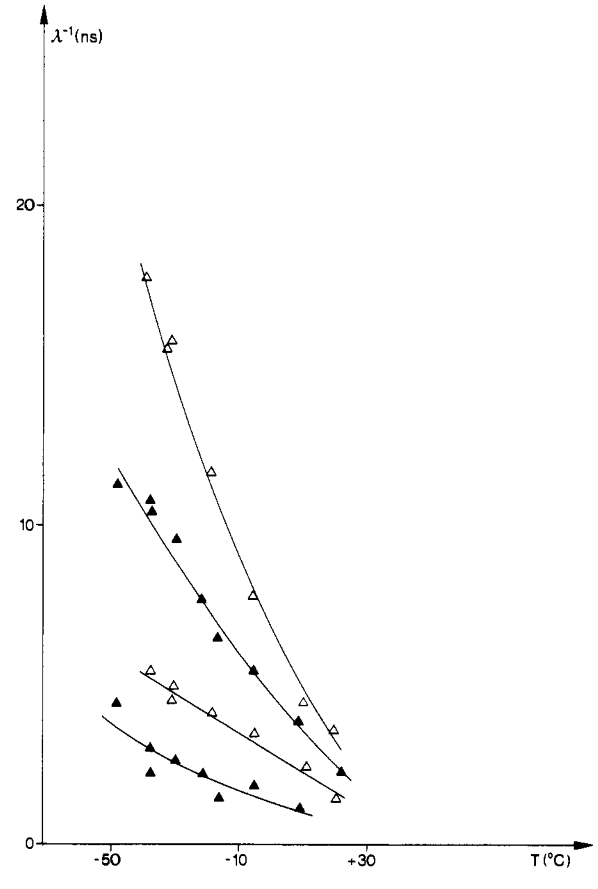

Figure 7. Fluorescence decay lifetimes of I in CH_3CN: ▲, monomer region; △, excimer region.

= 425 nm) was measured at various temperatures. In isooctane, the emission at 325 nm decays biexponentially between −50 and +10 °C. The lifetime of the longer living component $(\lambda_1^{325})^{-1}$, increases from 5 ns at +10 °C to 13.6 ns at −50 °C. The shorter living one, $(\lambda_2^{325})^{-1}$, varies from 2 ns at +10 °C to 6 ns at −50 °C (Figure 5). The analysis of the decay at 425 nm yields growing in times which correspond with neither component of the monomer region. Furthermore, the decay times of the excimer, varying from 9 ns at +10 °C to 24 ns at −50 °C, are longer than those of both components in the monomer region, indicating that there is no monomer component originating from return from the excimer. In such a case the *A* factor should be very large and should decrease with increasing temperature. This is clearly not the case, as can be seen in Figure 6.

At temperature above +10 °C, the lifetimes become too short to be measured accurately by the SPC equipment. In CH_3CN, similar results are obtained but the two lifetimes in the monomer region lie further apart, making the situation clearer than that in isooctane (Figure 7). It is more significant that the parameter related to the grow in of the excimer lies between those of the two monomer components. The ratio of the preexponential terms in the monomer region is almost constant in this solvent (Figure 6) and close to 1. Also in MTHF, an analogous picture emerged (Figure 8). In this latter solvent, the *A* factors are even seen to slightly decrease with decreasing temperature.

Photoproducts. Irradiation of I with $\lambda > 280$ nm yields the endo and exo cyclomers.[20] The endo cyclomer easily undergoes Cope rearrangement at a product with a conjugated double bond. The cyclomers can be reopened to I by irradiating with $\lambda < 254$ nm. Sensitization with benzophenone[21] yielded no reaction, proving that neither of the cyclomers is formed via the triplet excited state. To check whether the excimer fluorescence could be related specifically to one of the geometries of the products, we separated and froze the cyclomers in an ethanol matrix at 77

---

[20] R. Todesco, J. Gelan, H. Martens, J. Put, N. Boens, and F. C. De Schryver *Tetrahedron Lett.* **31**, 2815 (1978).

[21] C. A. Parker, "Photoluminescence of Solutions", Elsevier, Amsterdam, London, New York, 1968, p 92.

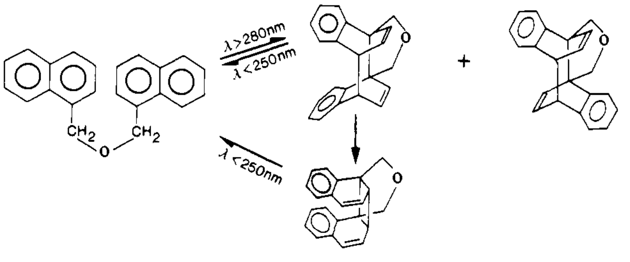

K. They were split by irradiation at 254 nm, and the fluorescence spectra of the obtained sandwich configurations were recorded. It is assumed that in the matrix only small motions are possible and that no conversion from the exo to the endo configuration can occur. Both split cyclomers yielded the same fluorescence spectrum with a maximum at 415 nm. It can be concluded that an exo and an endo excimer exist, with the same spectral distributions. In the exo excimer, a conformation with the two naphthyl groups in juxtaposition is impossible. They must be parallel but shifted with respect to each other. As both excimers have the same spectral distributions, we assume that the endo excimer has also a shifted configuration. This could be explained by accepting structures a and b for the respective excimers, in which the relative position of the two rings is almost the same.

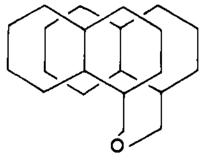

a

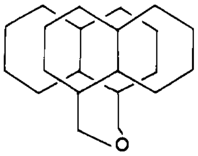

b

Chandross and Dempster[22] obtained only the endo cyclomer in the cyclomerization of 1,3-dinaphthylpropane, while in our case both cyclomers were obtained. Also, in the cyclomerization of 1,3-di-α-naphthylpropanol only the endo cyclomer[23] was obtained, proving that the difference in behavior is due to a conformational effect of the oxygen in the chain. This can easily be explained if the exo and endo excimers act as intermediates. In 1,3-dinaphthylpropane, there would be a severe interaction in the exo excimer between the hydrogens of the central methylene group and the α-hydrogen of one of the naphthyl groups. This interaction is absent in the endo excimer, and it is of course avoided in both excimers if there is an oxygen in the center of the linking chain. In the bis(α-naphthylmethyl) ether, the endo/exo ratio depends on the solvent and on the temperature (Table II). from these ratios and the quantum yields of product disappearance, we calculated the quantum yields for formation of the endo (ϕ_{rn}) and exo (ϕ_{rx}) cyclomers (Table II).

Kinetic Scheme. In Scheme I the decay parameter of the second exponential term in the time evolution of the monomer term in the time evolution of the monomer fluorescence must be identical with the decay parameter of the excimer fluorescence (this is λ_1 in eq 4 and 5). Experimentally this is not the case in isooctane, CH_3CN, and MTHF. Thus, the slow component of the decay at 310 is not due to dissociation of the excimer ($\lambda_1^{310} \neq \lambda_1^{420}$). An alternative explanation could be a competitive scheme, scheme II, in which a nonfluorescent species B and excimer D[24] are formed from excited monomer M. Relating ln k_3 to $1/T$ allows E_3 to be calculated from nonstationary measurements. This yields a value of 10.9 kJ/mol in isooctane, which is not in agreement with the value of 16.8 kJ/mol obtained from stationary results.

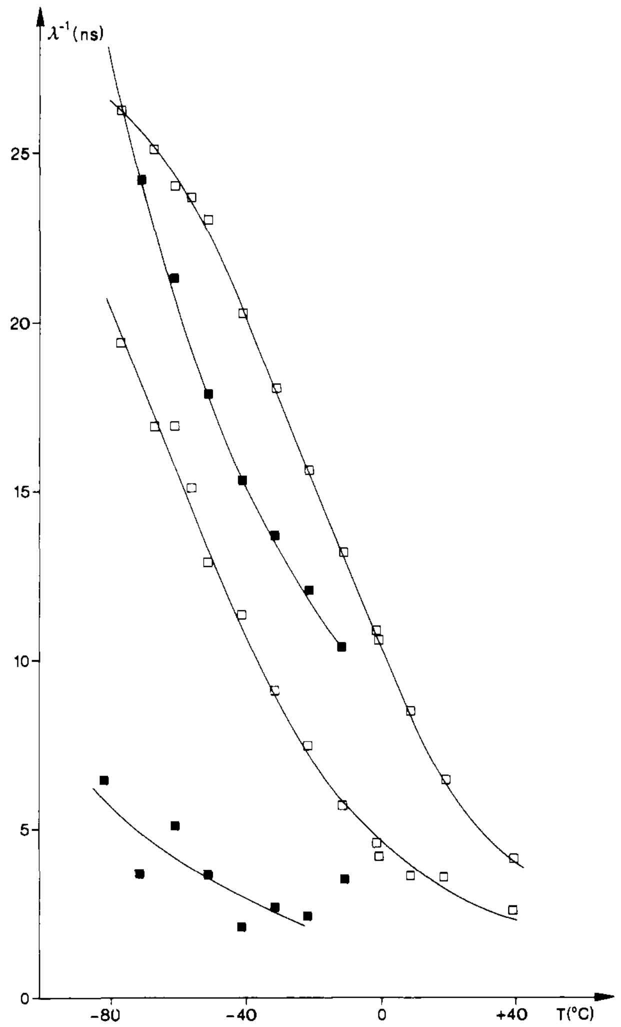

Figure 8. Fluorescence decay lifetimes of I in MTHF: ■, monomer region; □, excimer region.

Table II. Percentages and Quantum Yields of Endo and Exo Cyclomerization of 1

solvent	T, °C	% endo	% exo	ϕ_{rn}	ϕ_{rx}
isooctane	−10	42	58	0.0073	0.0100
	−30	37	63	0.0032	0.0055
	−50	22	78	0.0008	0.0027
	−70	16	84		
CH_3CN	−10	39	61	0.0110	0.0174
	−30	40	60	0.0092	0.0138
	−45	42	58	0.0053	0.0073
MTHF	−10	48	52	0.0099	0.0107
	−30	34	66	0.0037	0.0072
	−50	26	74	0.0018	0.0054
	−70	10	90		

Scheme II

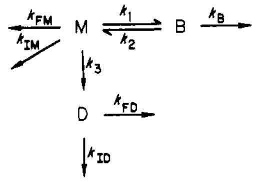

Another argument against Scheme II is based on the calculation of the ratio of the preexponential terms. This ratio of 21 at −40 °C in MTHF, which means that the growing in time constant of the excimer must practically equal $(\lambda_1^{310})^{-1}$. This is clearly not the case: the growing in of the excimer lies in between the parameters of the two monomer components (Figure 8). Furthermore with use of this model the entropy and enthalpy for the formation of B can be calculated on the basis of the experimental data, and both are found to be positive which is rather unlikely for complex formation. Two alternative schemes are based on

---

[22] E. A. Chandross and C. J. Dempster, *J. Am. Chem. Soc.*, **92**, 703 (1970).

[23] R. Todesco, J. Gelan, H. Martens, J. Put, and F. C. De Schryver, *Bull. Soc. Chim. Belg.* (1980).

[24] L. Aerts, Ph.D. Thesis K.U.L., 1979.

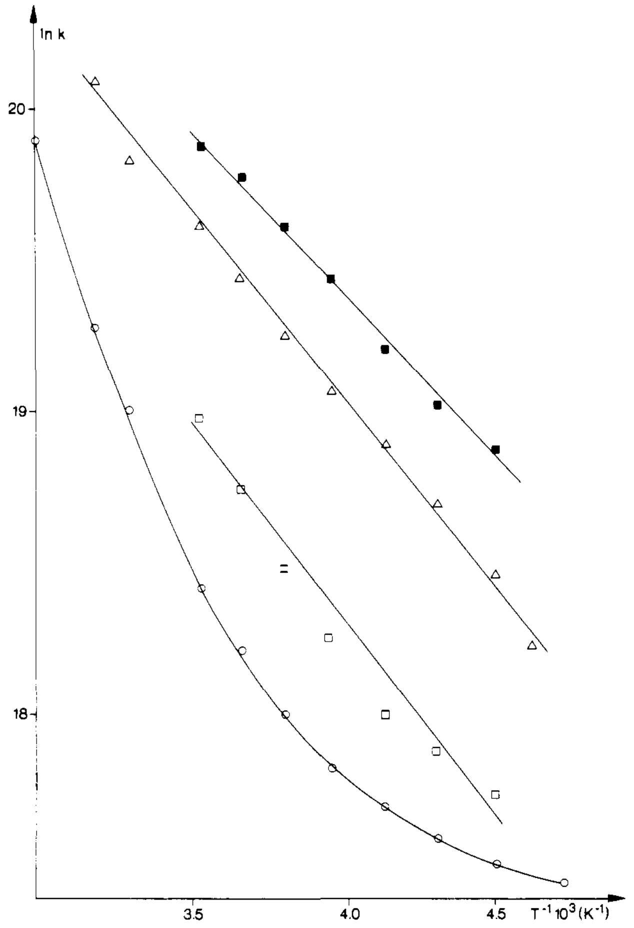

Figure 9. Arrhenius plot of the rate constants in isooctane: ■, k_F; △, k_{INC}; □, k_S; ○, k_D.

the assumption that there are two different sets of starting conformations which upon excitation can form excimers with a different rate.[11,12] This assumption leads to either a consecutive scheme or a competitive scheme. The consecutive scheme can be eliminated on the basis of the relation between the endo cyclomer/exo cyclomer ratios and the ratios of the preexponential factors in CH_3CN and MTHF (Table II and Figure 6). In CH_3CN, the A factors are almost constant and close to unity and so is the endo/exo ratio. In MTHF the A factors and the endo/exo ratios decrease slightly with decreasing temperature.

Furthermore it is obvious that exo and endo cyclomers cannot be formed from the same excimer.

The following facts must be taken into consideration while putting forward a scheme: both exo and endo cyclomers are formed and both these cyclomers yield the same excimer fluorescence in an ethanol matrix at 77 K; the decay in the monomer region consists of two components, neither of which coincides with that of the excimer (this means that two different species, fluorescing in the monomer region, must exist); the endo/exo cyclomer ratios are closely related to the A factors in the monomer region. All these facts can be explained by assuming two sets of conformations, differing in the relative orientation of the naphthyl groups and leading to the endo and exo excimers, respectively. These sets of conformations are considered to be in equilibrium in the ground state, but upon excitation, interconversion from one set to the other, within the lifetime of the excited state, is prohibited. This leads to Scheme III, where F and F* = ground state and first excited state of a set of conformations giving the endo excimer through a fast process, S and S* = ground state and first excited singlet state of a set of conformations giving the exo excimer through a slower process, D_1^*, D_2^* and D_1, D_2 = the endo and exo excimers and their respective ground states, k_M and k_D have the same meaning as in Scheme II, k_F and k_S = rate constants for the formation of the endo and exo excimers, respectively from the "fast" and "slow" conformations, and k_{-F} and k_{-S} = rate constants for the backreaction from the excimer to F* and S*. In the temperature region studied k_{-F} and k_{-S} are very small compared to k_D.

Scheme III

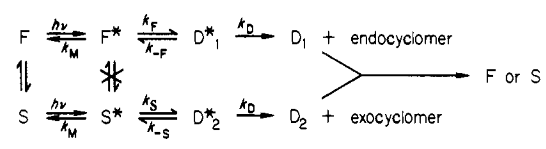

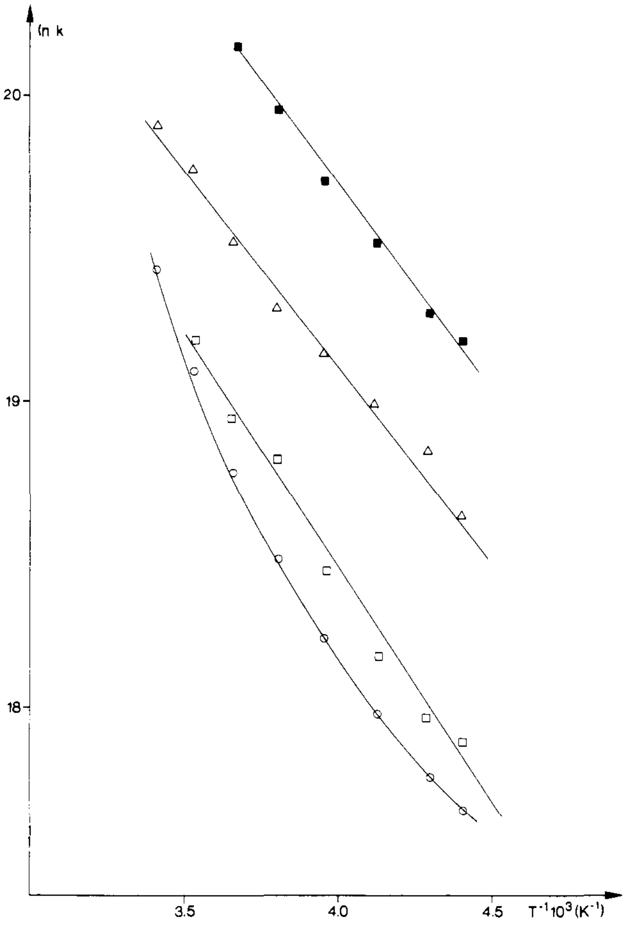

Figure 10. Arrhenius plot of the rate constants in CH_3CN: ■, k_F; △, k_{INC}; □, k_S; ○, k_D.

Within this scheme the time evolution of the emission of the excimer, $I_D(t)$ is given by eq 8,[12] where X_S = the fraction of

$$I_D(t) \approx \frac{X_s k_s}{k_D - k_S - k_M} e^{-(k_M+k_S)t} + \frac{X_F k_F}{k_D - k_F - k_M} e^{-(k_M+k_F)t} + \left(\frac{X_S k_S}{k_M + k_S - k_D} + \frac{X_F k_F}{k_M + k_F - k_D} \right) e^{-k_D t} \quad (8)$$

molecules in the fast set and X_F = the fraction of molecules in the slow set. The calculated values of the ratios of the preexponential terms of $e^{-(k_S+k_M)t}$ and $e^{-(k_F+k_M)t}$ using this scheme are found to be 1.74 in isooctane, 0.70 in MTHF, and 0.87 in CH_3CN, all at −30 °C. From these ratios it follows that the growing in of the excimer must be biexponential, leading to a three-exponential time evolution of the excimer fluorescence. As the growing in is shorter than the decay, it is stored in a small amount of channels in the SPC analysis. Treating the time evolution of the excimer fluorescence as a difference of two exponentials leads to a monoexponential growing in, yielding a lifetime which is a weighted average of the two monomer lifetimes. As one can see from Figures 5, 7 and 8, this is compatible with the fact that the growing of the excimer lies in between the lifetimes of the two

Table III. Activation Energies and Preexponential Terms of I in Isooctane, MTHF, and CH_3CN

solvent	E_F, kJ mol^{-1}	$10^{10}A_F$, s^{-1}	E_S, kJ mol^{-1}	$10^{10}A_S$, s^{-1}	E_{ID}, kJ mol^{-1}	$10^{12}A_{ID}$, s^{-1}	E_{FD}, kJ mol^{-1}	10^8A_{FD}, s^{-1}
isooctane	8.8	1.7	10.9	1.5	26.0	3.9	3.3	0.2
MTHF	6.7	1.0	10.0	0.7	21.7	0.8	2.9	0.1
CH_3CN	10.9	6.6	12.5	4.3	21.3	1.3	5.0	0.3

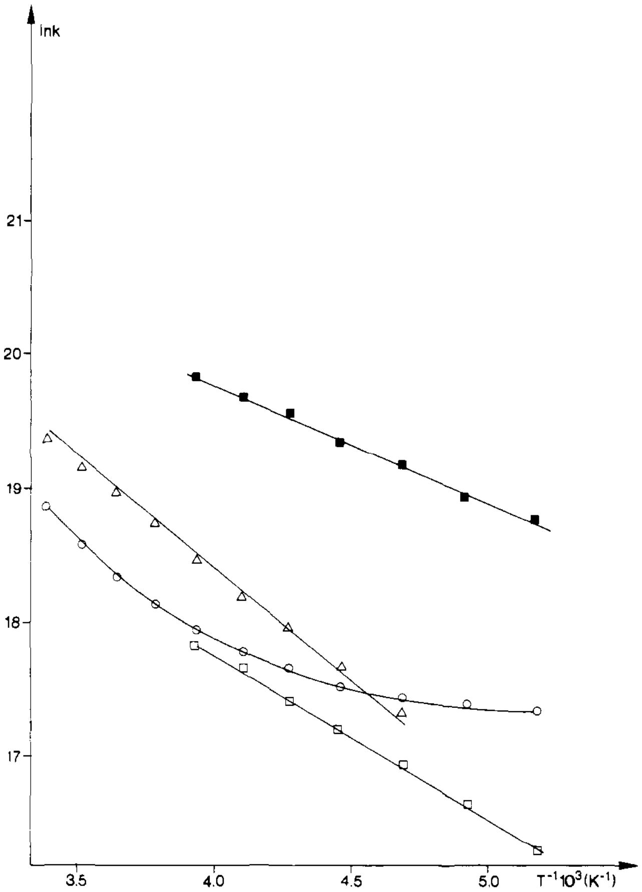

Figure 11. Arrhenius plot of the rate constants in MTHF: ■, k_F; △, k_{INC}; □, k_S; ○, k_D.

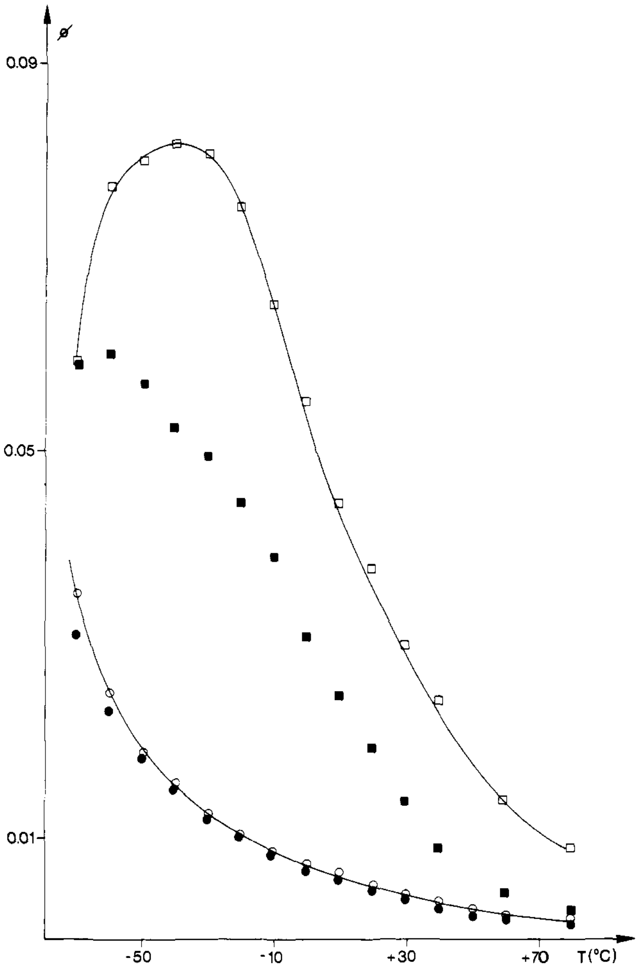

Figure 12. Calculated and experimental values of ϕ_{FM} and ϕ_{FD} in isooctane: ●, ϕ_{FM}(calcd); ○, ϕ_{FM}(exptl); ■, ϕ_{FD}(calcd); □, ϕ_{FD}(exptl).

monomer components. The rate constants in this scheme can be calculated from the experimental SPC data by using eq 9–12.[12]

$$1/\lambda_{2mon} = k_F + k_{FM} + k_{IM} \tag{9}$$

$$1/\lambda_{1mon} = k_S + k_{FM} + k_{IM} \tag{10}$$

$$1/\lambda_{1exc} = k_D = k_{FD} + k_{ID} \tag{11}$$

$$1/\lambda_{2exc} = k_{INC} = X_F k_F + X_S k_S \tag{12}$$

k_{FM} and k_{IM} ($k_{FM} + k_{IM} = k_M$) are obtained by analysis of the model compound at the same temperature. Here k_{INC} is the rate constant for the growing in of the excimer. The latter rate constant can be obtained directly from the experimental λ_2 in the excimer region or can be calculated by using eq 12. The two methods yield the same values which confirms the proposed mechanism. A plot of the logarithm of the rate constants k_F, k_S, k_{INC}, and k_D vs. the reciprocal of the temperature is shown in the Figures 9–11 for the solvents isooctane, CH_3CN, and MTHF, respectively. A linear relationship is found except for k_D. From these Arrhenius plots the activation energies E_F, E_S, E_{INC}, and E_{ID}[25] and the preexponential factors A_F, A_S, A_{INC}, and A_{ID} are obtained. Using the rate constants obtained from the experiments under nonstationary conditions, we can calculate back the quantum yields of monomer fluorescence and excimer fluorescence and compare them with the values obtained in the stationary measurements.

From the proposed kinetic scheme, one can derive eq 13 and 14. All the rate constants in eq 13 are known at various temperatures, so ϕ_{FM} can be calculated. The calculated and experimental values match exactly in all three solvents (Figures 12–14). In eq 14, k_{FD} is unknown. We calculated k_{FD} from the experimental ϕ_{FD} at the lowest temperature. Using this value of k_{FD}, we calculated ϕ_{FD} at other temperatures. As one can see in Figures 12–14, the calculated values are lower than the experimental ones. This could be explained by a temperature dependence of k_{FD}. A plot of ln k_{FD}, calculated with eq 14 from the experimental ϕ_{FD}'s vs. $1/T$, is linear in the three solvents (Figure 15). From this Arrhenius plot the activation energy E_{FD} and the preexponential factor A_{FD} are obtained. A temperature dependence of k_{FD} was found earlier by Hirayama and Lipsky[26] for the intermolecular

$$\phi_{FM} = k_{FM}\left(\frac{X_F}{k_M + k_F} + \frac{X_S}{k_M + k_S}\right) \tag{13}$$

$$\phi_{FD} = \frac{k_{FD}}{k_D}\left(\frac{X_F k_F}{k_M + k_F} + \frac{X_S k_S}{k_M + k_S}\right) \tag{14}$$

---

[25] R. B. Cundall and L. C. Pereira, *Chem. Phys. Lett.*, **15**, 383 (1972).

[26] F. Hirayama and S. Lipsky, *J. Chem. Phys.*, **51**, 1939 (1969).

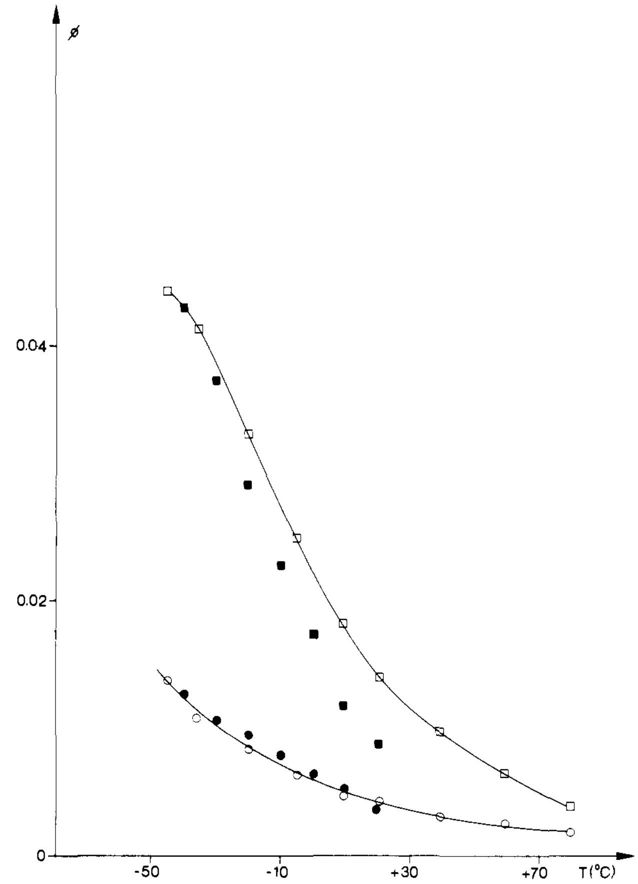

Figure 13. Calculated and experimental values of ϕ_{FM} and ϕ_{FD} in CH_3CN: ●, ϕ_{FM}(calcd); ○, ϕ_{FM}(exptl); ■, ϕ_{FD}(calcd); □, ϕ_{FD}(exptl).

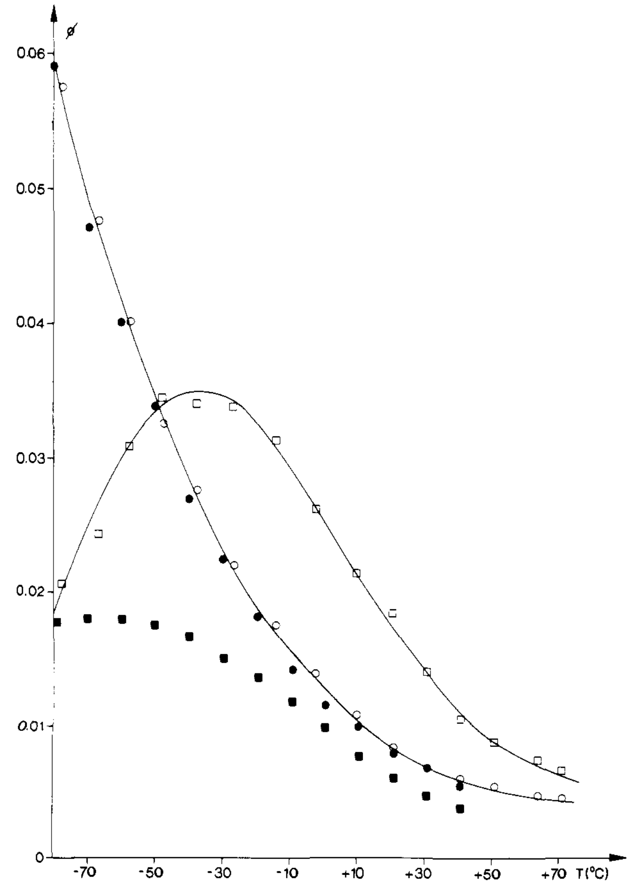

Figure 14. Calculated and experimental values of ϕ_{FM} and ϕ_{FD} in MTHF: ●, ϕ_{FM}(calcd); ○, ϕ_{FM}(exptl); ■, ϕ_{FD}(calcd); □, ϕ_{FD}(exptl).

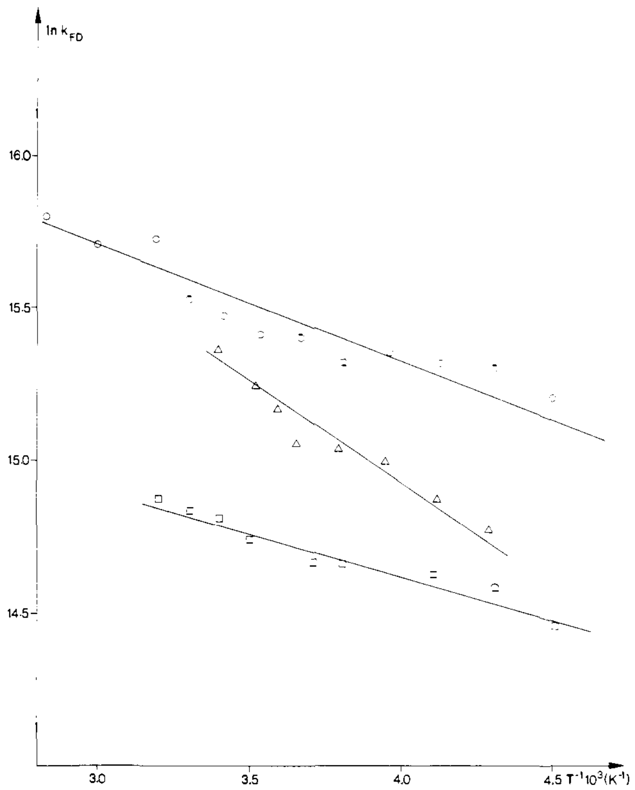

Figure 15. Arrhenius plot of k_{FD}: ○, isooctane; △, CH_3CN; □, MTHF.

excimer between two benzene molecules and two toluene molecules. This observation has been supported by Cundall and Robinson.[27] The temperature dependence of k_{FD} could be explained by the population of higher levels for vibration along the interchromophoric coordinates,[28] leading to a higher transition probability at higher temperatures. The activation energies and the preexponential terms of the various rate constants in the three solvents are summarized in Table III. From the results in Table III it is obvious that the interpretation of the Stevens–Ban plot on the basis of the stationary results is not valid. The interpretation of the tangent to the curve of ϕ_{FD}/ϕ_{FM} vs. $1/T$ is much more complex than was supposed. Equation 15 gives the expression for ϕ_{FD}/ϕ_{FM} according to this scheme.

$$\frac{\phi_{FD}}{\phi_{FM}} = \frac{k_{FD}k_F}{k_{FM}k_D}\left(\frac{k_S + k_M(X_F + X_S(k_S/k_F))}{k_M + X_Sk_F + X_Fk_S}\right) \tag{15}$$

Conclusion

Fluorescence measurements under nonstationary conditions suggest the importance of conformational effects on the intramolecular excimer formation. Two monomer components are seen which are most probably related to two sets of conformations, differing in the relative orientation of the naphthyl groups and leading to endo and exo excimers, respectively. These two sets of conformations are considered to be in equilibrium in the ground state, but upon excitation, interaction between the naphthyl groups prohibits interconversion from one set to the other. An excimer conformation was proposed in which the naphthalene rings are parallel but displaced, so that the position of the rings is the same in the endo and exo excimers.

Experimental Section

Absorption spectra were recorded on a Varian Techtron 635 or a Perkin-Elmer 124 double-beam spectrophotometer. Optical densities were measured with a Varian or a Hitachi spectrophotometer. Corrected emission spectra were run on a "Fica absolute and differential

---

[27] R. B. Cundall and D. A. Robinson, *Chem. Phys. Lett.*, **14**, 438 (1972).

[28] V. Yakhot, M. D. Cohen, and Z. Ludner, *Adv. Photochem.*, **11**, 489 (1979).

fluorometer" and excitation spectra on a "Spex Fluorolog". Temperature was controlled by a stream of nitrogen which was first passed through liquid nitrogen and then heated to the appropiate temperature. The concentration of the fluorescence species in the stationary and nonstationary measurements was 10^{-4} M. All samples were degassed by at least four freeze-thaw cycles. Decay measurements were performed by using the single-photon counting technique on an apparatus composed of Ortec and Canberra modules and an optical part of Applied Photophysics. The observed decays were deconvoluted by using a lamp spectrum and a nonlinear least-squares program. Bis(α-naphthylmethyl) ether and (α-naphthylmethyl) ethyl ether were prepared by a Williamson ether synthesis. Their purity was checked by analytical HPLC. Isooctane and acetonitrile were purchased from Merck (Uvasol) and used without further purification. Methyltetrahydrofuran was twice distilled over sodium hydride. None of the solvents used contained fluorescent contaminant upon excitation in the wavelength region of the experimental interest. Reaction quantum yields and endo/exo ratios were determined according to a method described in a previous paper.[29]

---

(29) N. Boens, M. De Brackeleire, J. Huybrechts, and F. C. De Schryver, *Z. Phys. Chem.* (*Wiesbaden*), **101**, 417 (1976).

Photochemical Processes of Benzophenone in Microheterogeneous Systems[†]

André M. Braun,*[1] Marianne Krieg,[2] Nicholas J. Turro, M. Aikawa, I. R. Gould, G. A. Graf, and Plato Chun-Chih Lee[3]

Contribution from the Institut de chimie physique, Ecole Polytechnique Fédérale de Lausanne, Ecublens, 1015 Lausanne, Switzerland, and the Department of Chemistry, Columbia University, New York, New York 10027.
Received May 5, 1981.
Revised Manuscript Received August 27, 1981

Abstract: The benzophenone triplet has been observed upon laser flash photolysis of the ketone solubilized in perfluorated micelles; its lifetime is found to be similar (7.87×10^{-6} s) to the value known from experiments in perfluorobenzene and perfluoromethylcyclohexane. Its $\epsilon_{TT}(\lambda_{max}$ 520 nm) of 2660 ± 380 L mol^{-1} cm^{-1} in sodium perfluorooctanoate (SPFO) and of 2460 ± 350 L mol^{-1} cm^{-1} in potassium perfluorooctylsulfonate (PPFOS) have been determined by using the method of Lachish et al. and assuming $\Phi_{isc} = 1$. Its phosphorescence is observed in perfluorated micelles ($\tau_{ph} = (7 \pm 3) \times 10^{-6}$ s), water ($\tau_{ph} = (12 \pm 4) \times 10^{-6}$ s), isooctane ($\tau_{ph} = (1.78 \pm 0.06) \times 10^{-6}$ s), and Freon 112 ($\tau_{ph} = (132 \pm 79) \times 10^{-6}$ s) with a striking resemblance of the weakly structured spectra (λ_{max} 445 nm) in the first two systems. The emission is quenched by nonfluorated surfactants such as sodium laurylsulfate (SLS) or cetyltrimethylammonium chloride (CTAC), presumably due to hydrogen abstraction; phosphorescence, triplet-triplet, and ketyl radical absorption transients are observed at concentrations of SLS above CMC, where the ketone should be nearly completely solubilized in a highly reactive micellar environment. Under micellar conditions, hydrogen abstraction occurs within the duration of our laser pulse (~30 ns). The kinetics of the triplet decay in perfluorated micelles as well as the decay of the ketyl radical, which results from hydrogen abstraction in SLS micelles, is strictly first order. Experiments in mixed micelles of SLS and SPFO indicate a faster decay of benzophenone triplets and a greater optical density of the signal component representing the corresponding ketyl radical when the mean occupancy number of SDS in SPFO is increased. The kinetics show a faster rate constant of hydrogen abstraction in those modelized micelles than in solutions of hydrocarbons. The solubilized ketyl radical may be deprotonated by an alkaline aqueous phase, and a cationic micelle clearly catalyzes this process. The lifetimes of ketyl radical and deprotonated ketyl radical anion are both longer in micellar systems than in homogenous solutions due to their isolation in surfactant aggregates.

During the last 20 years of active research in mechanistic photochemistry benzophenone has always been of particular interest, both as a chromophore, representing carbonyl triplets, and as a probe for the study of environmental reactivity.[4] Passing from homogeneous solutions to organized microheterogeneous systems, such as micelles, microemulsions, or vesicles,[5] the well-known hydrogen abstraction process of a carbonyl triplet[4] may answer as well questions about the structure of the aggregate and the position of the solubilizate[6] within the micellar aggregate.

Micelles have been employed as a means to isolate, and, thus, eventually stabilize reactive intermediates for the purpose of their characterization at ordinary temperatures as well as in order to influence well-known patterns of reactivity by applying experimental conditions which modify the reactivity of those intermediates.[6]

Both water and perfluorated solvents have been shown to be relatively inert with benzophenone triplets, and, thus, those homogeneous solutions served as standards for our measurements in micellar system.[7,8]

Experimental Section

Benzophenone of commercial grade has been recrystallized three times from ethanol, mp 48 °C.

Sodium perfluorooctanoate (SPFO) has been prepared from the corresponding carboxylic acid (perfluorooctanoic acid, PFO, FLUKA). A 0.024-mol sample of PFO in 45 mL of CH_3OH is mixed with an equivalent amount of NaOH in 45 mL of methanol, and the salt is precipitated by adding 170 mL of chloroform to the well-stirred solution. The precipitation is filtered, dried, and reprecipitated from a similar mixture of chloroform and methanol. Anal. Calcd: C, 22.04; Na, 5.27. Found: C, 22.0; Na, 5.11; H, <0.3.

Potassium perfluorooctanesulfonate (PPFOS) has been prepared by hydrolyzing perfluorooctanesulfonyl fluoride[9] with aqueous potassium

---

[†] Dedicated to George S. Hammond on the occasion of his 60th birthday.

(1) To whom correspondence should be addressed.

(2) Part of her thesis, EPFL, Lausanne, 1981.

(3) Part of his thesis, Columbia University, New York, 1980.

(4) N. J. Turro, "Modern Molecular Photochemistry", The Benjamin/Cummings Publishing Co.: Menlo Park, CA, 1978.

(5) J. H. Fendler, and E. J. Fendler, "Catalysis in Micellar and Macromolecular Systems", Academic Press: New York, 1975.

(6) N. J. Turro, M. Grätzel, and A. M. Braun, *Angew. Chem. Int. Ed. Engl.*, **19**, 675 (1980).

(7) (a) R. V. Bensasson and J.-C. Gramain, *J. Chem. Soc., Faraday Trans. 1*, **76**, 1801 (1980); (b) M. B. Ledger and G. Porter, ibid., **68**, 539 (1972). (c) D. M. Rayner and P. A. H. Wyatt, *J. Chem. Soc. Faraday Trans.* 2, **70**, 945 (1974).

(8) (a) D. I. Schuster, T. M. Weil, and A. M. Halpern, *J. Am. Chem. Soc.*, **94**, 8248 (1972). (b) C. A. Parker and T. A. Joyce, *Trans. Faraday Soc.*, **65**, 2823 (1969).

0002-7863/81/1503-7312$01.25/0